# Application of Electromagnetic Sensor in Electro-Pneumatic Actuator Displacement Control Under Variable Loads Conditions: Experimental Analysis

Noorhazirah Sunar[1*], M. F. Rahmat[1], Ahmad 'Athif Mohd Faudzi[2], Zool Hilmi Ismail[3], Siti Marhainis Othman[4], Siti Fatimah Sulaiman[5], Nur Haliza Abd Wahab[6]

[1*]School of Electrical Engineering, Faculty of Engineering, Universiti Teknologi Malaysia, Skudai, Johor Malaysia
[2] Center for Artificial Intelligence and Robotics, Universiti Teknologi Malaysia, Kuala Lumpur, Malaysia
[3] MJIIT, Department of System Electronic Engineering, Universiti Teknologi Malaysia, Kuala Lumpur, Malaysia
[4] Faculty of Electrical Engineering Technology, Universiti Malaysia Perlis (UniMAP), Perlis, Malaysia
[5] Center of Telecommunication Research and Innovation (CeTRI), Faculty of Electronics and Computer Engineering, Universiti Teknikal Malaysia Melaka, Melaka, Malaysia
[6] School of Computing, Faculty of Engineering, Universiti Teknologi Malaysia, Johor, Malaysia.

Corresponding author* email: noorhazirah@utm.my
Accepted 1 November 2021, available online December 2021

**ABSTRACT**

Dead-zone is a major issue that degrades the performance of the positioning control system in the pneumatic proportional valve control system. In order to address the issue, a switching inverse dead-zone compensator was incorporated to the pole-placement control of the Electro-Pneumatic Actuator (EPA) systems driven by a proportional directional control valve. The focus of this study is to do an experimental analysis to evaluate the robustness of the system under varying loads and varying position distances. Electromagnetic sensor is used to measure the displacement of the pneumatic cylinder piston movement. In this paper, the EPA model was chosen as a Hammerstein model that contains an Autoregressive with exogenous term (ARX) model and a nonlinear dead-zone model. The ARX model is estimated using the Recursive Least Square (RLS) method and the nonlinear model is obtained by using the Particle Swarm Optimization (PSO) method. The position tracking of the EPA system adapts to the pole-placement control law and is combined with switching inverse dead-zone in a feedforward manner. Experimental investigations were carried out for varying loads from 3.1 kg to 23.5 kg and varying position distances from 25 mm to 200 mm. Experimental results show that the EPA system controlled by the proposed controller is able to perform no overshoots for loads weighing less than 23.5 kg for all tested position distances. In addition, the proposed method achieved a steady state position error of 0.46 mm, a rise time of 0.21 s and a settling time of 0.49 s. The results demonstrated that as the load weight and position distance increased, transient time increased. However, the proposed method has successfully controlled the positioning of the EPA systems for all tested load weight and position distance.

**Keywords:** Dead-zone, Displacement Sensor, Pneumatic Actuator, Position Tracking, Proportional control Valve

## 1. Introduction

Pneumatic technology is essential in modern mechatronics systems [1]. One of the most common applications of pneumatics is the transfer of materials and loads over short distances [2]. and are frequently used in various industrial drives to achieve accurate position control [3]. Currently, over 70% of industrial servo control applications move objects weighing 1 to 10 kg [4]. In comparison to hydraulic and electrical actuators, pneumatic actuators have the following characteristics: good power density [2], speed output response, cleanness, cost, nonmagnetic [5], and simple operation mechanism [1]. The negative aspect of pneumatic technology is the significant nonlinearity of pneumatic drives, which has an impact on system dynamics [3]. Nonlinear behavior of pneumatic actuators in control applications is affected by dead zone of pneumatic valve [4], mass flow characteristics, friction force [2], and air compressibility [6].

For several decades, proportional directional control valves have been frequently employed in pneumatic servo systems [7]–[9]. The spool movement of a proportional direction valve is proportional to the input signal.

Accurate modeling is important to develop control for positioning of the EPA system. Basically, there are two methods to model the system: (1) theoretical analysis of nature's laws, and (2) the identification of the system model based on the measured input and output of the system. Not all the EPA system parameters are provided by the manufacturer. Furthermore, identifying the unknown parameters is time consuming. As a result, system identification has become a favorite among researchers. Numerous researchers developed the EPA model using system identification methods [10]–[13]. Autoregressive with exogenous (ARX), which is based on the principle of system identification, is notable for its ease of estimate and mathematical convenience [14]. To account for the EPA system's nonlinearity, the Hammerstein model structure is particularly well suited to represent the nonlinearity structure of the linear identification method [15], [16]. Additionally, the Particle Swarm Optimization (PSO) technique is literally appropriate for identifying parameters for nonlinear structures. To identify the Hammerstein model with non-minimum phase features, a PSO technique was investigated [17]. Several techniques for positioning control of the EPA system have been investigated such as nonlinear sliding mode control [18], fault tolerant and diagnosis method [1], [19], adaptive neural network [7], [20], [21], and predictive fuzzy control [22]. The aforementioned controllers, however, have control design issues such as measurement noise [23], complex controller architecture, and the need for more sensors as feedback element units. However, in this study, a pole-placement controller was selected since it is suited for discrete time systems and can be adapted to a polynomial system. Moreover, the closed-loop characteristics of the pole-placement influence the system's transient response and system's stability. The pole-placement controller has been successfully applied to the EPA systems [24]. Unfortunately, the offered techniques did not account for the dead-zone effect. In [7], it was discovered that the dead-zone characteristics limit the control accuracy.

The problem of dead zones is critical in the proportional control field of an electro-pneumatic controlled system with a proportional valve [25]. Nonlinearity in the dead zone degrades control performance and leads to instability. To reduce the impact of dead zones, inverse function-based techniques are utilized. In [25], [26] propose a nonlinear adaptive dead-zone compensator. Another method for minimizing the dead-zone effect is by adding the dead-zone in cascade with the linear control inputs. A 2DOF controller with a dead-zone compensator has been proposed in [5]. Another inverse dead-zone compensator for a nonlinear Proportional-Integral-Derivative (PID) controller has been investigated [27]. The inverse dead-zone compensator with a fuzzy self-adaptive PID controller was addressed in [28]. The proposed method was tested with a 3 kg payload, yielding a settling time of 0.83 seconds and an overshoot of 0.0146 mm. It has been demonstrated that the inverse dead-zone can solve the dead-zone issue. It also proved that the combination of the linear and dead-zone compensators reduces the influence of the dead-zone nonlinearity. A cascading dead-zone compensation was reported in the reviewed literature. Furthermore, the discontinuous dead-zone model leads to controller output chattering. The preceding technique does not take into consideration the discontinuity of the inverse dead-zone model. In this paper, a pole-placement controller with an inverse dead-zone compensation is employed in a feedforward approach. To reduce the chattering effect, a switch function and a parameter were introduced.

The following is how this paper is structured. Section 2 presents a model identification of the EPA system that takes into account the dead-zone nonlinearity. Followed by Section 3, the proposed method of switch inverse dead-zone function with the 2DOF pole-placement controller. The findings of the position control experiments are presented in Section 4. In this section, the proposed method was evaluated for varying position distances and varying loads to determine its efficacy. Finally, there is a conclusion to the current findings and a suggestion for further research.

## 2. Model Identification

To identify the mathematical model of the EPA system, the Hammerstein model is used. It consists of a linear dynamic element and a static nonlinear element. The static nonlinear element in this study is the EPA system's dead-zone model. While, the linear dynamic element is an ARX model.

### 2.1 System Description

Figure 1 depicts the EPA system used to conduct this study. The system comprises of a personal computer, a 500 mm double acting pneumatic cylinder, an Enfield bidirectional proportional valve, a National Instrument data acquisition card, and a Jun-Air Compressor. During system operation, the EPA system communicates with the computer using the MATLAB Real Time Window target.

q

(b)

Figure 1. Electro-pneumatic actuator system test bed

### 2.2 Identification of ARX Model

The SI MATLAB toolbox is used to estimate the linear ARX model. The rich frequencies input $u(t)$ described in (1) are used to excite the EPA system.

$$u(t) = 0.8\cos cos\,(2\pi\times 0.05t) + 0.5cos(2\pi\times 0.2t) + 3\cos cos\,(2\pi\times 0.05t) \quad (1)$$

$$y(t) = \frac{B(z)}{A(z)}r(t) + e(t) \quad (2)$$

### 2.3 Identification of Dead-Zone Model

The dead-zone can be expressed as the relationship between input, $u_d(t)$ and output, $u(t)$ of the proportional valve as in (3) and depicted in Figure 2. From Figure 2, $b_r$ and $b_l$ are the right break point and left breakpoint respectively. Meanwhile, $m_r$ and $m_l$ are the right slope and left slope in Figure 2. The particle swarm optimization technique is used to estimate parameters $b_r$, $b_l$, $m_r$, and $m_l$.

$$u_d(t) = m_l u(t) - m_l b_l\; u(t) < b_l\; 0\; b_l \leq u(t) \leq b_r\; m_r u(t) - m_r b_r\; u(t) > b_r \quad (3)$$

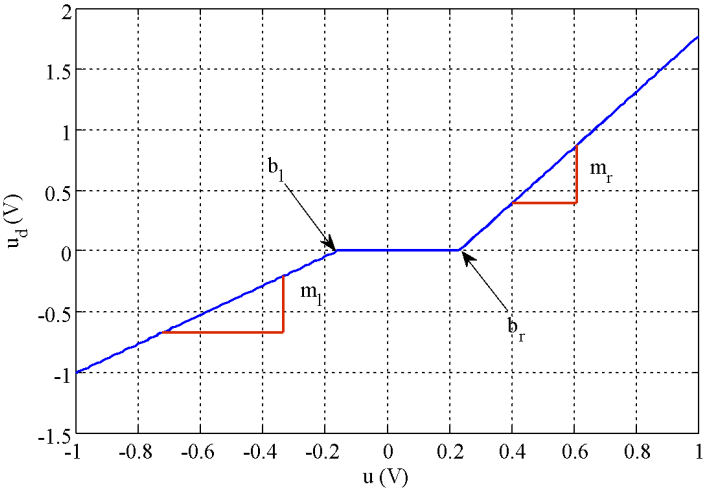


Figure 2. Asymmetry dead-zone model

## 3. Controller Design

In this study, the proposed controller is designed in two parts. First, the linear part, which is developed based on pole-placement control law. Second, the nonlinear part, which is a switching function based on the inverse dead-zone model.

### 3.1 Two-Degree of Freedom (2DOF) Pole Placement Controller

The Two-Degree of Freedom (2DOF) Pole-Placement controller is used in this paper for position tracking of the EPA system. The 2DOF pole-placement controller is shown in Figure 3. From Figure 3, the 2DOF pole-placement controller consists of output compensation and input compensation. The controller output $u(t)$ is given in (4).

$$u(t) = \frac{H(z)}{F(z)} r(t) + \frac{G(z)}{F(z)} y(t) \tag{4}$$

Where time, $t$ is the number of samples, $n$ multiplied by sampling time,$T_{sample}$ ($t = nT_{sample}$), $r(t)$ is reference input, and $y(t)$ is position output. Meanwhile $H(z)$, $F(z)$, and $G(z)$ is a polynomial $z^{-1}$ and can be expressed as:

$$F(z) = 1 + f_1 z^{-1} + \ldots + f_{n_f} z^{-n_f} \tag{5}$$

$$G(z) = g_0 + g_1 z^{-1} + \ldots + g_{n_g} z^{-n_g} \tag{6}$$

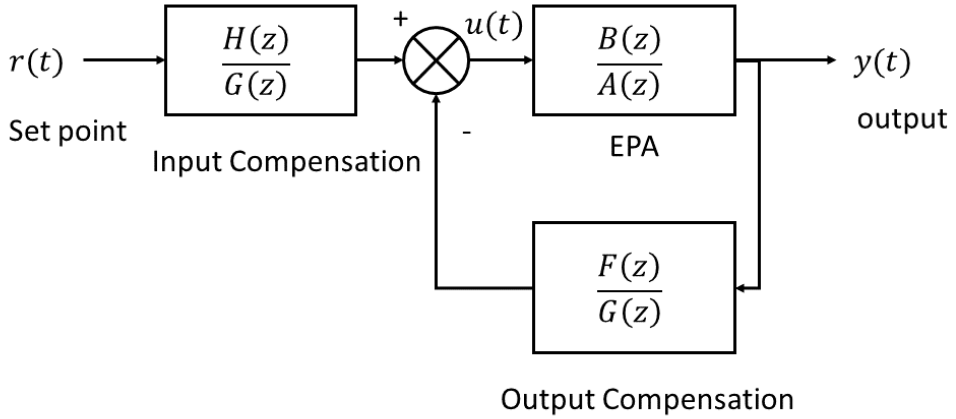


Figure 3. The 2DOF pole-placement controller block diagram

The system's closed loop can be expressed as in equation (7):

$$y(t) = \frac{B(z)H(z)}{A(z)F(z)+B(z)G(z)}r(t) \tag{7}$$

Let the characteristics of the system $T(z)$ is given by equation (8) for the closed loop system in equation (7), and the diophantine equation be defined as equation (9).

$$T(z) = 1 + t_1 z^{-1} + \ldots + t_{n_t} z^{-n_t} \tag{8}$$

$$A(z)F(z) + B(z)G(z) = T(z) \tag{9}$$

Then, the value of $H(z)$ can be calculated as follows:

$$H(z) = \frac{T(z)}{B(z)}\Big|_{z=1} \tag{10}$$

### 3.2 2DOF Pole-placement Controller with Switching Inverse Dead-Zone Compensator

As illustrated in Figure 4, the switching compensator based on the inverse dead-zone model was introduced as a feedforward to the output of the pole-placement controller. The compensator's output is expressed as follows:

$$u_{ff}(t) = lc\left(\frac{1}{m_r}u(t) + b_r\right)SE.DE + lc\left(\frac{1}{m_l}u(t) + b_l\right)SE.\overline{DE} \tag{11}$$

The dead-zone compensator act as a switch function in this paper. It is activated when the error between output position, $y(t)$ and the references input, $r(t)$ is in the steady-state error, $(SE)$. The $lc$ parameter is introduced to reduce the chattering effect. In equation (11) consists of two components: the right inverse dead-zone component and the left inverse dead-zone component. When the direction error, $(DE)$ is positive the right component is active and when the $DE$ is negative, the left component is active.

Figure 4. The 2DOF pole-placement controller with switching inverse dead-zone block diagram

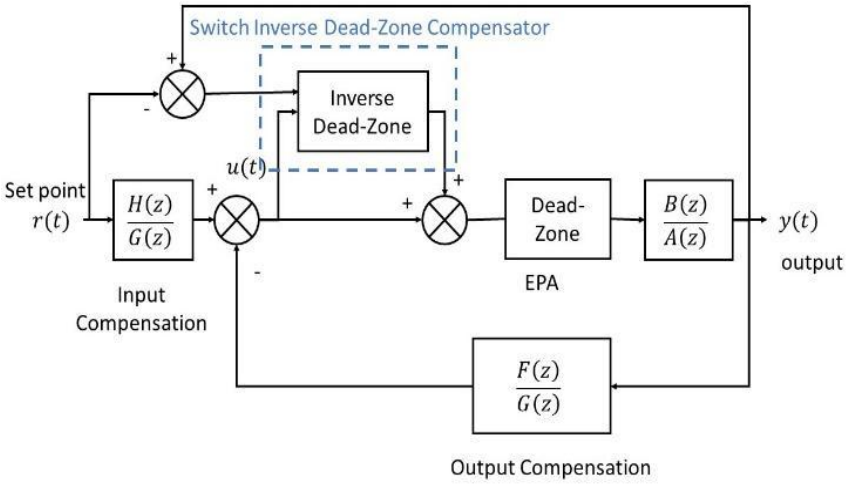


## 4. Results and Discussion

The experiments were carried out to evaluate the efficacy of the proposed controller in the real-time EPA system. As the use of the EPA system's positioning tracking involves moving the load from one place to another, the proposed controller is evaluated at various weights and position distances. The weights vary from 3.1 kg, 5.2 kg, 8.2 kg, 13.5 kg, and 23.5 kg and the position distances vary from 25 mm, 50 mm, 100 mm, and 200 mm. The following subsection represents the experimental results for the mentioned conditions and the steady-state error ($e_{ss}$), the overshoots ($OS\%$), the rise time ($T_r$), and the settling time ($T_s$) are recorded.

.

### 4.1 Vary Set Point

Three control algorithms are compared in order to further validate the proposed controller's efficacy. The first controller is a traditional pole-placement controller (PP). This is to demonstrate the importance of the dead-zone compensator in the EPA system. The pole-placement controller with nonlinear dead zone compensation is the second controller. The dead-zone is cascaded with the output of the pole-placement controller in this controller. It functions as a dead-zone cancellation in EPA systems. The proposed controller, as described in the preceding section, is the third controller. The described three controllers were evaluated for tracking a step function with a position distance of 100 mm, and experimental results are shown in Figure 5.

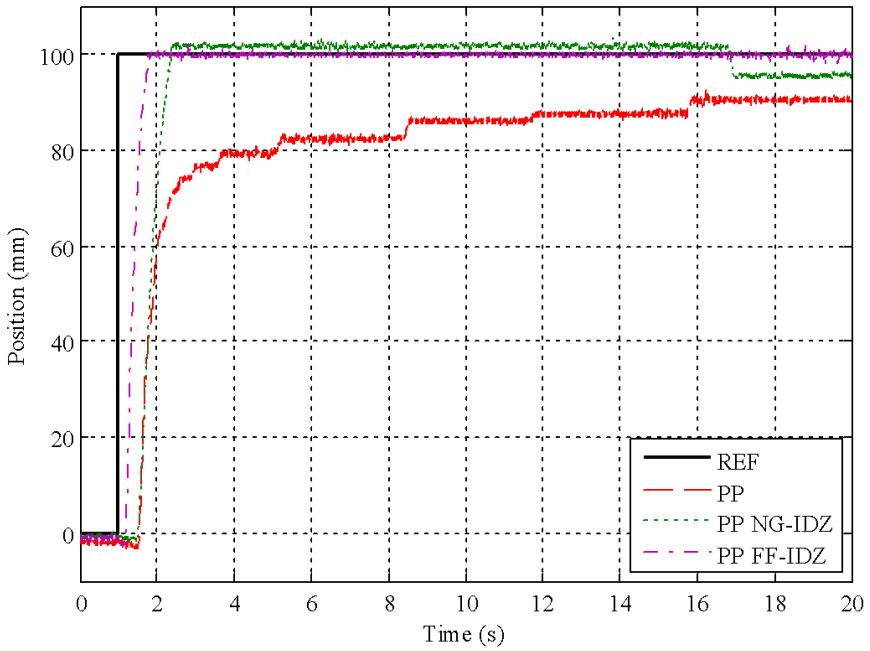


Figure 5. Experimental controller performance comparison for PP, NGIDZ and FFIDZ controller

As can be observed, the average tracking error of NGIDZ and FFIDZ is significantly lower than PP, indicating that valve dead-zone compensation is required. The average tracking error of FFIDZ and NGIDZ are 0.46 mm and 2.43 mm. These results indicate that the FFIDZ improved 96.9% of the steady-state error without a dead-zone compensator and 81.1% of the steady-state error with a nonlinear gain dead-zone compensator. In terms of time responses, it is noticeable that the proposed controller improved the NGIDZ and PP controllers' rising and settling times. The FFIDZ controller reduced the NGIDZ controller's rising time by 63.5 percent and its settling time by 42.2 percent. It was discovered that the feedforward inverse dead-zone controller successfully enhanced the performance of the cascade inverse dead-zone controller.

### 4.2 Vary Load at 25 mm Position

Figure 6 shows the result of the proposed controller tested at a 25 mm position distance for varying loads. The recorded criteria performances are tabulated in Table 1. It is clearly shown that an overshoot of 16% only occurred when attached to a 23.5 kg load. From Table 1, as the load increases, the transient time performance faster. The minimum error is 0.48 mm and the maximum error is 0.67 mm.

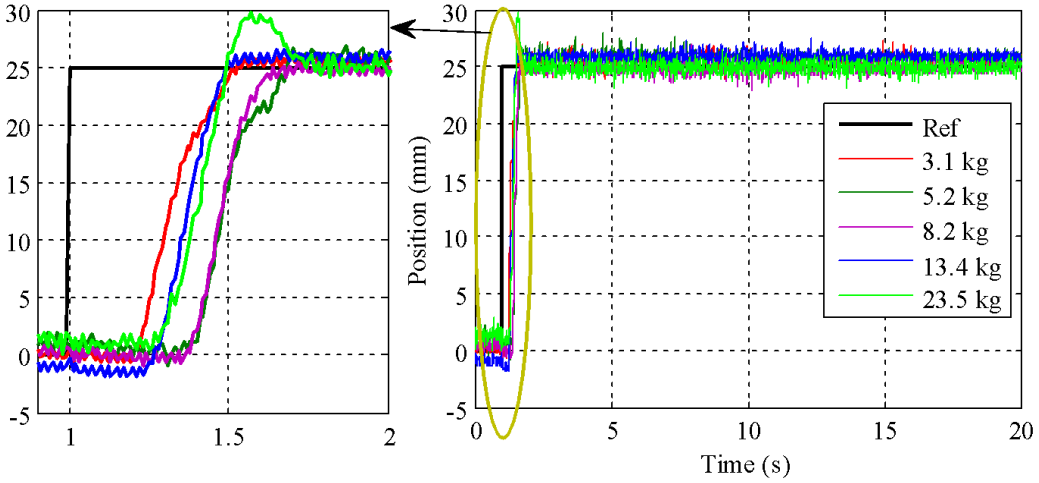


Figure 6. Experimental controller performance for 25 mm at varying loads

**Table 1.** Controller performance for 25 mm position distance at varying load

| Criteria | Rise time (s) | Settling Time(*s*) | Steady-state error (mm) | Overshoot (%) |
|---|---|---|---|---|
| 3.1 kg | 0.24 | 0.51 | 0.67 | 0 |
| 5.2 kg | 0.23 | 0.66 | 0.99 | 0 |
| 8.2 kg | 0.18 | 0.61 | 0.48 | 0 |
| 13.4 kg | 0.17 | 0.49 | 0.97 | 0 |
| 23.5 kg | 0.8 | 0.49 | 0.59 | 16 |

### 4.3 Vary loads at 50 mm Position

Figure 7 captures the results of proposed controller tested at a 50 mm position distance and the performances are recorded in Table 2. Similar to the results at a 25mm, the overshoots of 12% only occurred when the proposed controller tested at a 23.5 kg load. Compared to 25 mm position distance, the 50 mm position distance displays increased maximum position error at 3.01 mm while the minimum position error remains at 0.48mm. However, there is no trend or relationship between transient time and load. The transient time demonstrates fluctuate trend as load increased.

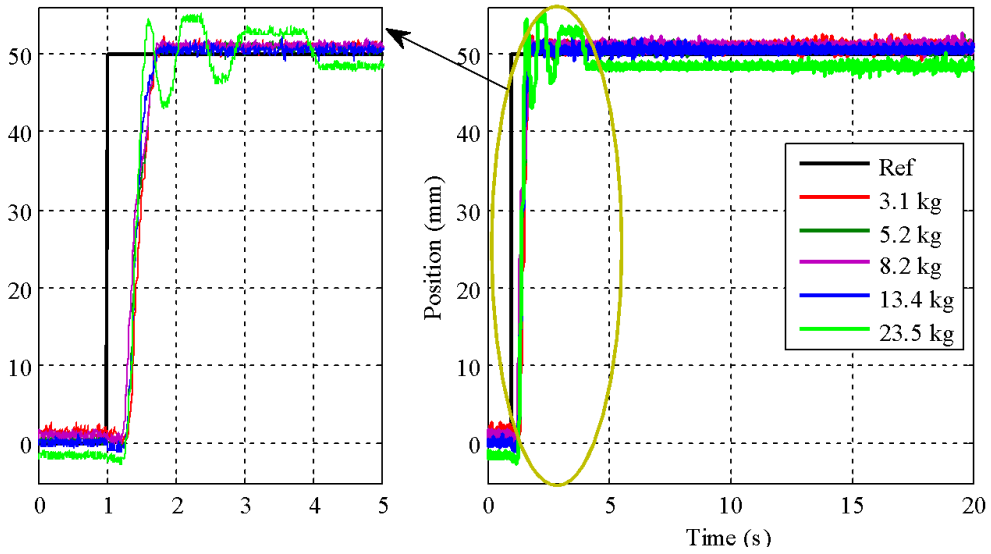


Figure 7. Experimental controller performance for 50 mm at varying loads

**Table 2.** Controller performance for 50 mm position distance at varying load

| Criteria | Rise time (s) | Settling Time(*s*) | Steady-state error (mm) | Overshoot (%) |
|---|---|---|---|---|
| 3.1 kg | 0.30 | 0.72 | 1.04 | 0 |
| 5.2 kg | 0.32 | 0.54 | 0.48 | 0 |
| 8.2 kg | 0.37 | 0.69 | 0.81 | 0 |
| 13.4 kg | 0.26 | 0.69 | 0.81 | 0 |
| 23.5 kg | 0.19 | 0.70 | 3.01 | 12 |

### 4.4 Vary Load at 100 mm Position

The position distance was increased to 100 mm and is illustrates in Figure 8 and the criteria performance is tabulated in Table 3. Referring to the Table 3, the overshoots of 2.7% appear at 13.4 kg loads and at 23.5 kg loads shows 16.9% overshoot. The maximum position error is 3.01 mm and minimum position error is 0.46 mm. For 50 mm position distance, as the load tested increases, the transient time increase.

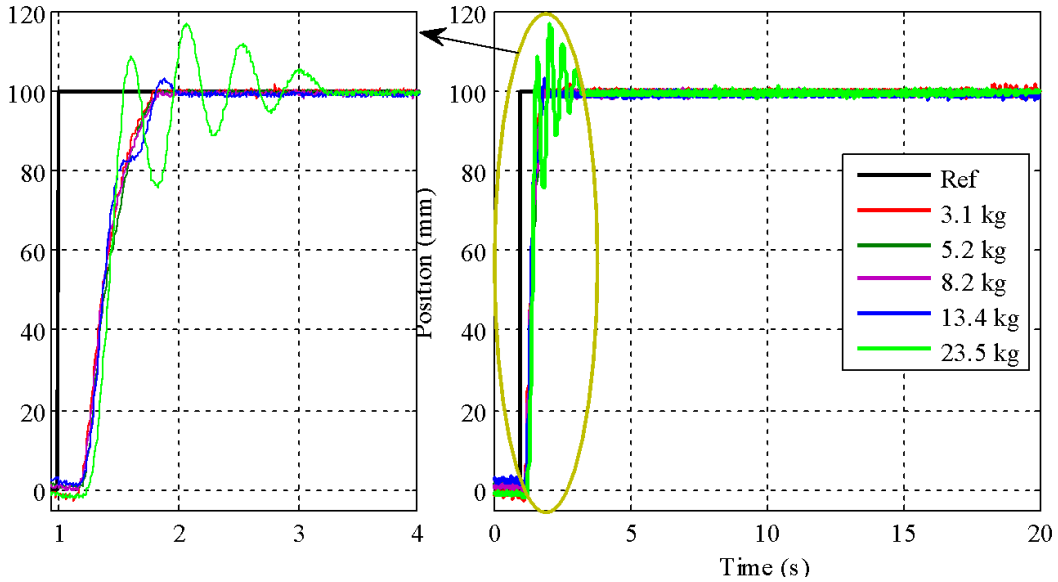


Figure 8. Experimental controller performance for 100 mm at varying loads

**Table 3.** Controller performance for 100 mm position distance at varying load

| Criteria | Rise time (s) | Settling Time(*s*) | Steady-state error (mm) | Overshoot (%) |
|---|---|---|---|---|
| 3.1 kg | 0.41 | 0.78 | 0.46 | 0 |
| 5.2 kg | 0.41 | 0.82 | 0.46 | 0 |
| 8.2 kg | 0.44 | 0.82 | 0.81 | 0 |
| 13.4 kg | 0.48 | 0.82 | 0.81 | 2.7 |
| 23.5 kg | 0.21 | 1.55 | 3.01 | 16.9 |

### 4.5 Vary Load at 200 mm Position

Finally, the proposed controller was tested to a 200 mm position distance. Figure 9 shown the results of the proposed controller at varying load and the criteria performances is recorded in Table 3. From Table 3, the overshoots of the system, occurred at 23.5 kg load. The maximum position error is 1.43 mm and the minimum position error is 1.43 mm. The transient time increased as the load increases.

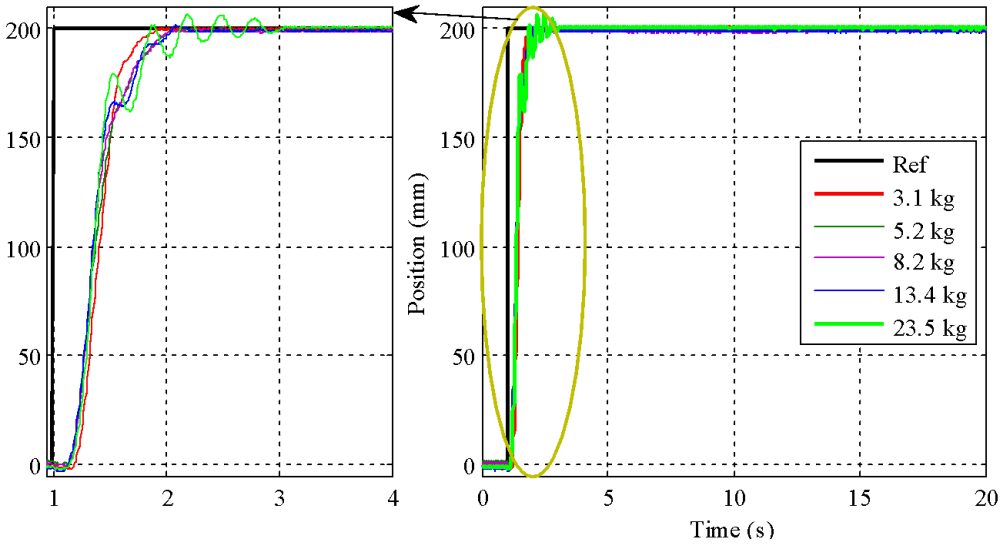


Figure 9. Experimental controller performance for 200 mm at varying loads

**Table 3.** Controller performance for 200 mm position distance at varying load

| Criteria | Rise time (s) | Settling Time(*s*) | Steady-state error (mm) | Overshoot (%) |
|---|---|---|---|---|
| 3.1 kg | 0.34 | 0.81 | 0.51 | 0 |
| 5.2 kg | 0.50 | 0.86 | 0.77 | 0 |
| 8.2 kg | 0.50 | 1.04 | 1.43 | 0 |
| 13.4 kg | 0.52 | 1.05 | 1.13 | 0 |
| 23.5 kg | 0.54 | 1.04 | 1.33 | 3.05 |

For the overall evaluated distance, the steady state error exhibits spike position error at 23.5 kg load for 50 mm and 100 mm position error. Others, not display spike position error. The maximum steady state error of 1.43 mm and minimum error of 0.46 mm. Overall time response performance for distances less than or equal to 25 mm; as the evaluated load increased, the time response decreased. Meanwhile, as we increased the position distance, the time response rose in proportion to the evaluated load. According to the overall results, the proposed method's performance is capable of exhibiting no overshoots for loads less than 23.5 kg, with a maximum overshoot of 16.9 %.

Similar to the relations between transient time and load analysis that have been discusses in previous subsection, the transient time increase as the position distance increase. These results exhibits that the positions distance and loads influence the transient time performance. As the load increased, the momentum to start and stop the mass increased. This is the reason the rise time and settling time increased as the loads and position distance increased.

## 5. Conclusion

This paper focus on experimental study of the proposed method at varying loads and varying position distance. The proposed controller are tests for 3.1 kg, 5.2 kg, 8.2 kg, 13.4 kg and 23.5 kg loads. Also, the proposed controller are tests for position distance 25 mm, 50 mm, 100 mm and 200 mm. The experimental results demonstrated that the load and position distance influence the transient time and the overshoot of the position tracking of the EPA systems. In terms of the effectiveness of the proposed controller, the proposed controller improved the transient response, steady state error and overshoot of the pole-placement with cascade inverse dead-zone compensator. In comparison with reported controller in the literature review, for load 3kg, the proposed controller improved the settling time and overshoot of the fuzzy self-adaptive PID controller. In this paper, the model identification and controller design of the

proposed controller depends only on position transducer which reduced the numbers of sensor and cost in positioning the EPA system. In order to improve the robustness of the EPA system, gain scheduling for load and position distance based can be a solution for the future work in positioning accuracy of the EPA system.

## Acknowledgment

This research was supported by the research University Grant (GUP) Tier 1 vote number Q.J130000.7123.00H36. We would like to express our gratitude to our colleagues who contributed insight and expertise that greatly assisted the research.

## References

[1] A. Tootchi and A. Chaibakhsh, "Fault Tolerant Control for Trajectory Tracking of a Pneumatic Servo Positioning System," in *2018 6th RSI International Conference on Robotics and Mechatronics (IcRoM)*, 2018, pp. 53–58, doi: 10.1109/ICRoM.2018.8657629.

[2] G. V Kreinin, S. Y. Misyurin, N. Y. Nosova, and M. V Prozhega, "Parametric and Structural Optimization of Pneumatic Positioning Actuator," in *Advanced Technologies in Robotics and Intelligent Systems*, 2020, pp. 395–403.

[3] D. Saravanakumar, B. Mohan, and T. Muthuramalingam, "A review on recent research trends in servo pneumatic positioning systems," *Precis. Eng.*, vol. 49, pp. 481–492, 2017, doi: https://doi.org/10.1016/j.precisioneng.2017.01.014.

[4] C.-R. Rad and O. Hancu, "An improved nonlinear modelling and identification methodology of a servo-pneumatic actuating system with complex internal design for high-accuracy motion control applications," *Simul. Model. Pract. Theory*, vol. 75, pp. 29–47, 2017, doi: https://doi.org/10.1016/j.simpat.2017.03.008.

[5] Y. Shirato, W. Ohnishi, and T. Koseki, "Two-Degree-of-Freedom Control with Adaptive Dead Zone Compensation for Pneumatic Valves," *Samcon2019*, no. 11, pp. 1–6, 2019.

[6] Z. Zhang, S. Wang, J. Kan, W. Hu, Z. Chen, and H. Xu, "A pneumatic piezoelectric vibration energy harvester based on the compressed air-transducer-structure interaction," *Energy Convers. Manag.*, vol. 213, p. 112861, 2020, doi: https://doi.org/10.1016/j.enconman.2020.112861.

[7] Y. Chen, G. Tao, and F. Meng, "An Intelligent Adaptive Robust Controller Based on Neural Network for a Pneumatic System," *{IOP} Conf. Ser. Mater. Sci. Eng.*, vol. 575, p. 12016, Aug. 2019, doi: 10.1088/1757-899x/575/1/012016.

[8] S. Liu, Q. Sun, Z. Chen, and F. Dong, "Characteristic Model-based Generalized Predictive Control for Electro-hydraulic System with Dead-zones and Parameter Uncertainty∗∗This work is supported by the National Natural Science Foundation of China under Grant 61273138, 61573197 and the Science & T," *IFAC-PapersOnLine*, vol. 51, no. 20, pp. 287–294, 2018, doi: https://doi.org/10.1016/j.ifacol.2018.11.027.

[9] M. I. P. Azahar, A. Irawan, and R. M. T. R. Ismail, "Self-tuning hybrid fuzzy sliding surface control for pneumatic servo system positioning," *Control Eng. Pract.*, vol. 113, p. 104838, 2021, doi: https://doi.org/10.1016/j.conengprac.2021.104838.

[10] A. Messina, N. I. Giannoccaro, and A. Gentile, "Experimenting and modelling the dynamics of pneumatic actuators controlled by the pulse width modulation (PWM) technique," *Mechatronics*, vol. 15, no. 7, pp. 859–881, 2005, doi: https://doi.org/10.1016/j.mechatronics.2005.01.003.

[11] I. M. Yassin, M. N. Taib, and R. Adnan, "Recent advancements \& methodologies in system

identification: A review," *Sci. Res. J.*, vol. 1, no. 1, pp. 14–33, 2013.
[12] M.-C. Shih and S.-I. Tseng, "Identification and position control of a servo pneumatic cylinder," *Control Eng. Pract.*, vol. 3, no. 9, pp. 1285–1290, 1995, doi: https://doi.org/10.1016/0967-0661(95)00127-G.
[13] Y. Wang, D. Tao, J. Li, and G. Bao, "Research on variable gain feedforward trajectory control of pneumatic servo system," in *2015 International Conference on Fluid Power and Mechatronics (FPM)*, 2015, pp. 350–354, doi: 10.1109/FPM.2015.7337138.
[14] A. K. Tangirala, "Identification of dynamic models--concepts and principles," *Princ. Syst. Identif. Theory Pract.*, pp. 479–518, 2014.
[15] J. Chen, X. Wang, and R. Ding, "Gradient based estimation algorithm for Hammerstein systems with saturation and dead-zone nonlinearities," *Appl. Math. Model.*, vol. 36, no. 1, pp. 238–243, 2012, doi: https://doi.org/10.1016/j.apm.2011.05.049.
[16] S. F. Sulaiman, M. F. Rahmat, A. A. M. Faudzi, K. Osman, N. H. Sunar, and S. N. S. Salim, "Hammerstein model based RLS algorithm for modeling the intelligent pneumatic actuator (IPA) system," *Int. J. Adv. Sci. Eng. Inf. Technol.*, vol. 7, no. 4, pp. 1457–1463, 2017.
[17] H. N. Al-Duwaish, "Identification of Hammerstein Models with Known Nonlinearity Structure Using Particle Swarm Optimization," *Arab. J. Sci. Eng.*, vol. 36, no. 7, pp. 1269–1276, 2011, doi: 10.1007/s13369-011-0120-2.
[18] Y.-C. Tsai and A.-C. Huang, "FAT-based adaptive control for pneumatic servo systems with mismatched uncertainties," *Mech. Syst. Signal Process.*, vol. 22, no. 6, pp. 1263–1273, 2008, doi: https://doi.org/10.1016/j.ymssp.2007.10.011.
[19] A. Andrade, K. Lopes, B. Lima, and A. Maitelli, "Development of a Methodology Using Artificial Neural Network in the Detection and Diagnosis of Faults for Pneumatic Control Valves," *Sensors*, vol. 21, no. 3, 2021, doi: 10.3390/s21030853.
[20] Y. Chen, G. Tao, and H. Liu, "High Precision Adaptive Robust Neural Network Control of a Servo Pneumatic System," *Appl. Sci.*, vol. 9, no. 17, 2019, doi: 10.3390/app9173472.
[21] H.-P. Ren, S.-S. Jiao, J. Li, and Y. Deng, "Adaptive neural network control of pneumatic servo system considering state constraints," *Mech. Syst. Signal Process.*, vol. 162, p. 107979, 2022, doi: https://doi.org/10.1016/j.ymssp.2021.107979.
[22] S. Mu, S. Goto, S. Shibata, and T. Yamamoto, "Intelligent position control for pneumatic servo system based on predictive fuzzy control," *Comput. Electr. Eng.*, vol. 75, pp. 112–122, 2019, doi: https://doi.org/10.1016/j.compeleceng.2019.02.016.
[23] S. Riachy and M. Ghanes, "A Nonlinear Controller for Pneumatic Servo Systems: Design and Experimental Tests," *IEEE/ASME Trans. Mechatronics*, vol. 19, no. 4, pp. 1363–1373, 2014, doi: 10.1109/TMECH.2013.2280956.
[24] Y. Shirato, W. Ohnishi, H. Fujimoto, T. Koseki, and Y. Hori, "Controller design of mass flow rate loop for high-precision pneumatic actuator," in *2020 IEEE 16th International Workshop on Advanced Motion Control (AMC)*, 2020, pp. 40–45, doi: 10.1109/AMC44022.2020.9244409.
[25] D. Meng, A. Li, B. Lu, C. Tang, and Q. Li, "Adaptive Dynamic Surface Control of Pneumatic Servo Systems With Valve Dead-Zone Compensation," *IEEE Access*, vol. 6, pp. 71378–71388, 2018, doi: 10.1109/ACCESS.2018.2881305.
[26] L. Chen and Q. Wang, "Finite-time adaptive neural dynamic surface control for non-linear systems with unknown dead zone," *IET Control Theory \& Appl.*, 2020.
[27] S. N. S. Salim, M. F. Rahmat, L. Abdullah, S. A. Shamsudin, M. Zainon, and A. F. M. Amin, "Enhanced self-regulation nonlinear PID for industrial pneumatic actuator," *Int. J. Electr. Comput. Eng.*, vol. 9, no. 4, p. 3015, 2019.

[28] M. I. P. Azahar, A. Irawan, and R. M. Taufika, "Fuzzy Self-Adaptive PID for Pneumatic Piston Rod Motion Control," in *2019 IEEE 10th Control and System Graduate Research Colloquium (ICSGRC)*, 2019, pp. 82–87, doi: 10.1109/ICSGRC.2019.8837064.